REPORT DOCUMENTATION PAGE

AFRL-SR-AR-TR-04-

0019

1. REPORT DATE *(DD-MM-YYYY)*	2. REPORT TYPE	3. DATES COVERED *(From - To)*
29-11-2003	Final Technical Report	15-08-2002 - 29-11-2003

4. TITLE AND SUBTITLE
Atomic Layer Deposition of Oxidizer Coatings on Aluminum Nanoparticles to Fabricate Superthermite Explosives

5a. CONTRACT NUMBER
F49620-02-C-0058

5b. GRANT NUMBER

5c. PROGRAM ELEMENT NUMBER

6. AUTHOR(S)
Buechler, Karen, J
George, Steven, M
Ferguson, John

5d. PROJECT NUMBER

5e. TASK NUMBER

5f. WORK UNIT NUMBER

7. PERFORMING ORGANIZATION NAME(S) AND ADDRESS(ES)

ALD NanoSolutions, Inc.
11711 Chase Ct.
Westminster, CO 80020

University of Colorado
The Regents of the University
Of Colorado, 572 UCB
Boulder, CO 80309

8. PERFORMING ORGANIZATION REPORT NUMBER

9. SPONSORING / MONITORING AGENCY NAME(S) AND ADDRESS(ES)
AFOSR
4015 Wilson Blvd Room 713
Arlington, VA 22203

10. SPONSOR/MONITOR'S ACRONYM(S)

11. SPONSOR/MONITOR'S REPORT NUMBER(S)

12. DISTRIBUTION / AVAILABILITY STATEMENT
Approved for Public Release, Distribution Unlimited

20040130 073

13. SUPPLEMENTARY NOTES

14. ABSTRACT

Report developed under STTR contract for topic AF02T007. The primary goal of this research is to establish the technical feasibility of using atomic layer deposition to produce composite thermite particles. Secondary goals were to establish the conditions for deposition of tin oxide, coat a quantity of aluminum particles with tin oxide, characterize and test the coated particles, design a larger scale system for deposition, and evaluate the economic feasibility of the process. Chemistry to deposit tin oxide on zirconia particles by atomic layer deposition was successfully developed. This established conditions to shift the chemistry to the desired aluminum particle substrate. Composite thermite particles were synthesized through this surface growth of tin oxide and were shown to be highly reactive. However, deposition was not as efficient on the aluminum particles as the zirconia particles. The measured reactivity is less than theoretically expected, however the tested particles had an atomic ratio of oxygen to aluminum of 0.28 instead of the optimum 1.5. The reactivity falls off rapidly as this ratio deviates from optimum. The process can be economically scaled in a fluidized bed with a cost of coating the particles estimated as $9/kg with a capital investment of $500,000.

15. SUBJECT TERMS
STTR Report

16. SECURITY CLASSIFICATION OF:			17. LIMITATION OF ABSTRACT	18. NUMBER OF PAGES	19a. NAME OF RESPONSIBLE PERSON
a. REPORT	b. ABSTRACT	c. THIS PAGE			Karen Buechler
U	U	U	UU	21	19b. TELEPHONE NUMBER *(include area code)* (720) 840-1610

Abstract

Report developed under STTR contract for topic AF02T007. The primary goal of this research is to establish the technical feasibility of using atomic layer deposition to produce composite thermite particles. Secondary goals were to establish the conditions for deposition of tin oxide, coat a quantity of aluminum particles with tin oxide, characterize and test the coated particles, design a larger scale system for scale-up, and evaluate the economic feasibility of the process. Chemistry to deposit tin oxide on zirconia particles by atomic layer deposition was developed. This established condition to shift the chemistry to the desired aluminum particle substrate. Composite thermite particles were synthesized through this surface growth of tin oxide and were shown to be highly reactive. The measured reactivity is less than theoretically expected, however the tested particles had an atomic ratio of oxygen to aluminum of 0.28 instead of the optimum 1.5. The reactivity falls off rapidly as this ratio deviates from optimum. The process can be economically scaled with a cost of coating the particles estimated as $9/kg with a capital investment of $500,000.

Executive Summary

There are several goals of this work. The primary goal is to establish the technical feasibility of using atomic layer deposition to produce composite thermite particles. Secondary goals were to establish the conditions for deposition of tin oxide, coat a quantity of aluminum particles with tin oxide, characterize and test the coated particles, design a larger scale system for scale-up, and evaluate the economic feasibility of the process.

The chemistry for tin oxide growth was developed on zirconia nanoparticles of similar size to the aluminum nanoparticles. Growth was performed at 250 °C and proceeded in a controlled and expected manner. Transmission electron micrographs indicated that the film was conformal to the zirconia particles. As was expected for a crystalline material, the film appeared rough. The roughness was a function of film thickness as crystallites grew during film growth. Inductively coupled plasma atomic emission spectroscopy indicated the tin content of the composite particles was as expected based on literature reported growth rates and thicknesses from the micrographs.

Tin oxide growth onto the as received aluminum nanoparticles proceeded differently from on the zirconia particles. Micrographs of the films did not demonstrate as uniform of a coating as the films on the zirconia particles. Additionally, emission spectroscopy results indicated much lower growth rates of the tin oxide onto the aluminum particles at the same conditions. As a result additional conditions for growth were attempted on the aluminum particles; however these variations did not significantly improve the growth of the films. It is likely that the deposition is inhibited by some surface species on the surface of the particles as received.

The composite thermite particles were tested for reactivity through both qualitative and quantitative means. A small sample of both the aluminum and the composite particles were ignited with a tesla coil and the resulting reaction was video taped with a hand held digital video camera. The particles without coating reacted relatively slowly, producing a bright glowing mound. The composite particles reacted very rapidly, with a bright flash, sparks, a loud popping noise, and a mushroom cloud of smoke resulting from the ignition.

For quantitative results, a sample of composite material was sent to Dr. Steven Son at Los Alamos National Laboratory. The pressure increases observed during the ignition of the SnO_2-coated Al particles were only 3 – 5 % of their optimized energetic materials. The material tested has an O/Al molar ratio of 0.28, much lower than the stoichiometric 1.5 ratio for the thermite reaction. As these materials become less chemically ideal, the energy release falls off rapidly, explaining the low energy releases observed in this study.

A pilot scale fluidized bed system was designed and costs approximately $500,000 installed. The system designed would have the capacity to coat 100,000 kg of aluminum per year. Initial economic modeling of this fluidized bed system indicated that at full production rates, the tin oxide coating can be applied profitably for about $9/kg. This cost is strongly affected by capital costs and annual production rates. Operating and fixed costs are not strong variables in the current economic model of the coating process.

It is the recommendation that further work on this project progress on two parallel tracks. One track is to refine the tin oxide chemistry onto the aluminum particles. It is believed that additional work to establish safe protocols for scaling the energetic materials above the sub-gram quantities is needed. Experts in the energetics community would be contacted to advise on this track of work. The second track is to construct the designed pilot scale facility to begin investigating the large scale coating of nanosized particles by atomic layer deposition. Initial large scale trials on non-energetic systems such as tin oxide on zirconia or commercially important systems such as surface modified boron nitride for electronic packaging filler materials or tin oxide coated barium titanate for the multilayer capacitor industry will determine if atomic layer deposition on particles can be scaled up to full production volumes.

Background

High energy materials have many uses as explosives and propellants. Most high energy materials contain a fuel and an oxidizer. In the case of a conventional explosive, such as trinitrotoluene (TNT), the fuel and oxidizer are contained in the same molecule. In the case of a conventional thermite explosive, such as Al and Fe_2O_3, the fuel and oxidizer are mixed together in a powder composite. Because the diffusion distance between the fuel and oxidizer is large in the powder composite, e.g. $\sim 10^4$-10^5 nm, the explosive reaction velocity is slow, e.g. $\sim 10^{-1}$ m/s [1]. In contrast, because the diffusion distance between the fuel and oxidizer is small in a conventional explosive, e.g. ~1 nm, the explosive reaction velocity is fast, e.g. $\sim 10^3$ m/s [1]. Higher reaction velocities yield higher explosive power.

Although conventional thermite explosives have a slow reaction velocity, they release much more energy than conventional explosives. TNT has a reaction enthalpy of $\Delta H \sim 1.6$ kcal/cm^3. In comparison, the Al and Fe_2O_3 thermite reaction yields a much higher reaction enthalpy of $\Delta H \sim 3.9$ kcal/cm^3. This higher reaction enthalpy would lead to a much higher reactive power if there was a shorter diffusion distance and closer contact between the fuel and the oxidizer. To minimize diffusion distances and achieve this higher reactive power, nanostructured composites of Al and Fe_2O_3 have been fabricated using sol-gel methods [2]. In addition, nanoscale powders of Al and MoO_3 have been prepared and mixed to create a nanocomposite [3]. With particles sizes from 200-500 Å, nanopowdered mixtures of Al and MoO_3 display an explosive reaction velocity of more than 1000 times faster than conventional powdered thermites [3]. Additional studies have revealed that increasing the number of contact points between the fuel and oxidizer further increases the reaction velocity [4].

Ultrathin and conformal coatings can be deposited on nanoparticles using atomic layer deposition (ALD) techniques [5]. ALD is based on sequential, self-limiting surface reactions. The repetition of those surface reactions can produce ultrathin and uniform coatings with a thickness accuracy of ~1 Å on nanoscale particles. Recent reviews report that many materials, including a variety of oxides, can be deposited using ALD methods [6]. In addition, recent studies have also shown that the deposition can be conducted at a growth rate of ~1 Å every 5 seconds. Consequently, ALD has become a viable method to grow ultrathin and conformal films on a variety of surfaces.

ALD techniques are able to deposit the oxidizer directly on the fuel nanoparticle. Earlier work at the University of Colorado has demonstrated that conformal coatings of Al_2O_3 and SiO_2 with thicknesses of 25-100 Å can easily be deposited on nanometer-sized BN particles [7,8]. This degree of control and conformality will allow a stoichiometric amount of oxidizer to be deposited directly on the fuel nanoparticle. This precise stoichiometry will also enhance the reaction enthalpy per volume because neither the oxidizer nor fuel will be rate-limiting since each will be reacted to completion. Large quantities of particles can be coated by utilizing a fluidized particle bed ALD reactor [9]. By scaling up the size of the fluidized particle bed reactor, the ALD method can yield commercial quantities of coated particles.

The ALD method provides a unique opportunity to deposit uniform and conformal oxidizer coatings on fuel particles to fabricate an "all-in-one" superthermite particle. Various

combinations of fuel and oxidizer are possible to define the superthermite particle [10,11]. Since Al_2O_3 has one of the highest heats of formation of any metal oxide, most thermite reactions employ Al as the metal fuel. The oxidizer is typically a metal oxide with a much lower heat of formation than Al_2O_3. Various oxidizers can be employed such as Fe_2O_3, MoO_3, Co_3O_4, NiO, MnO_2, WO_3, CuO and SnO_2 [11]. Of the different oxidizers that can be utilized for thermite reactions, ALD methods have been used to deposit NiO [12], WO_3 [13], Co_3O_4 [14], MnO_2 [15] and SnO_2 [16].

Experimental

A schematic of the ALD coating reactor is shown in Figure 1. The gas dosing lines utilize bubblers to deliver precursors to the reactor. Automated valves will allow the carrier gas to alternatively pass through a bubbler for dosing or bypass a bubbler for purging. For example, if the valves labeled A_3 are closed and A_4 is open, the carrier gas will bypass Bubbler A to purge the reactor. Simultaneously opening the A_3 valves and closing the A_4 valve will divert the flow through the bubbler so that precursor A is entrained in the carrier gas and dosed to the reactor. Computer controls of these valves allow for operation of this system with reproducible sequences of dosing A, purging, dosing B, and final purging.

Two reactors have been used in this study. The prototype of the particle bed reactor was made from 3/8" glass tubing glued to 2 ¾" Conflat flanges. Metal filters (Mott Corp., average pore diameter 10 μm) were pressed into the Conflat flanges at both the top and bottom of the reactor to keep the particles in the bed. This glass reactor was necessary to observe the fluidization of the particles during gas flow and establish acceptable fluid dynamics in the reactor. However, this type of reactor with glass/metal interfaces would not withstand the heating required for the ALD reactions of interest. For the purpose of coating particles using ALD, a second reactor was constructed entirely from stainless steel. An illustration of this reactor is shown in Figure 2.

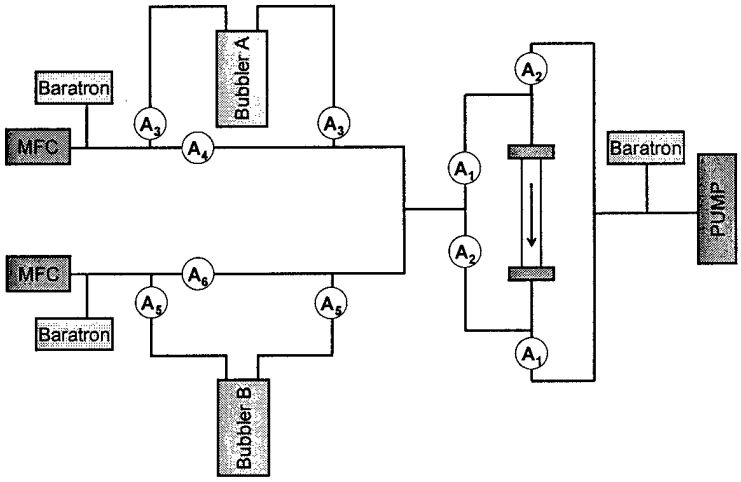

Figure 1 Diagram of ALD particle coating system.

Gas flow velocities in excess of 1 m/s and volumetric flow rates up to 700 sccm were used to fluidize the aluminum particles. Under these conditions, the aluminum particles were significantly agitated. When the automated gas valves were switched so that the gas flow was in the upward direction, the particles would become fluidized. A portion of the particles would

eventually become stuck on the top filter. Switching the gas valves to reverse the gas flow direction, a backpulse, would remove the particles on the upper filter and return them to the bottom of the particle bed reactor. The subsequent switch to upward flow would again fluidize the particles. The employment of this gas switching sequence would result in the repetition of fluidizing particles and then removing particles stuck on the upper filter.

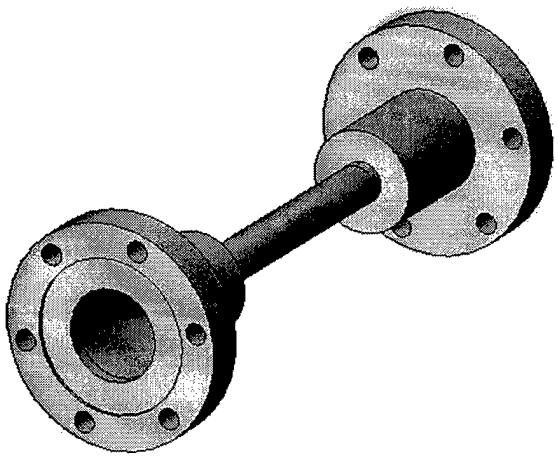

Figure 2 Drawing of steel particle ALD reactor.

A range of conditions were used to deposit SnO_2 on the aluminum particles. Approximately 0.5g of Al powder was used during each deposition. Reactor temperatures were 250 or 350 °C. The argon carrier gas was flowing at ~7.5 sccm through each mass flow controller for a total flow of 15 sccm. The sequence used for dosing the $SnCl_4$ precursor consisted of: (1) backpulse, (2) dose $SnCl_4$, (3) short purge, (4) backpulse, (5) dose $SnCl_4$, and (6) long purge. A similar sequence was used to dose the H_2O_2 precursor and consisted of: (1) backpulse, (2) dose H_2O_2, (3) short purge, (4) backpulse, (5) dose H_2O_2, and (6) long purge. The $SnCl_4$ and H_2O_2 were alternately dosed in an ABAB… sequence to deposit SnO_2. The backpulse time was 1s. The precursor dose times varied from 1 – 3s. The short and long purge times were typically 5 and 30s, respectively. The longer purge times between $SnCl_4$ and H_2O_2 were necessary to prevent chemical vapor deposition. The number of reaction cycles used to deposit SnO_2 varied from 250 – 1000.

Results and Discussion

Due to the explosive nature of SnO_2/Al composites, it was decided to first demonstrate ALD of SnO_2 on ZrO_2 particles. The ZrO_2 particles used for this study were obtained from Nanomaterials Research Corporation (Longmont, CO). These ZrO_2 particles were spherical with an average diameter of ~60 nm. Previous studies using transmission Fourier transform infrared (FTIR) spectroscopy and transmission electron microscopy (TEM) have shown these ZrO_2 particles to be ideal substrates for many types of ALD.

Tin oxide was deposited on the ZrO_2 particles using sequential exposures to $SnCl_4$ and H_2O_2/H_2O. The particles were in the stainless steel reactor, which was maintained at 250 °C. The ZrO_2 particles were subjected to 70, 140 or 500 $SnCl_4/H_2O_2$ cycles. After SnO_2 was deposited on the ZrO_2 particles, inductively coupled plasma – atomic emission spectroscopy (ICP-AES) and TEM were used to evaluate the SnO_2 coatings on the ZrO_2 particles.

The ICP-AES results for a variety of samples are shown in Figure 3. This plot shows the concentration of Sn in the samples (ppm) versus the number of $SnCl_4/H_2O_2$ cycles that the ZrO_2 particles were exposed to. In general, Figure 3 illustrates that the concentration of Sn increases with the number of $SnCl_4/H_2O_2$ cycles.

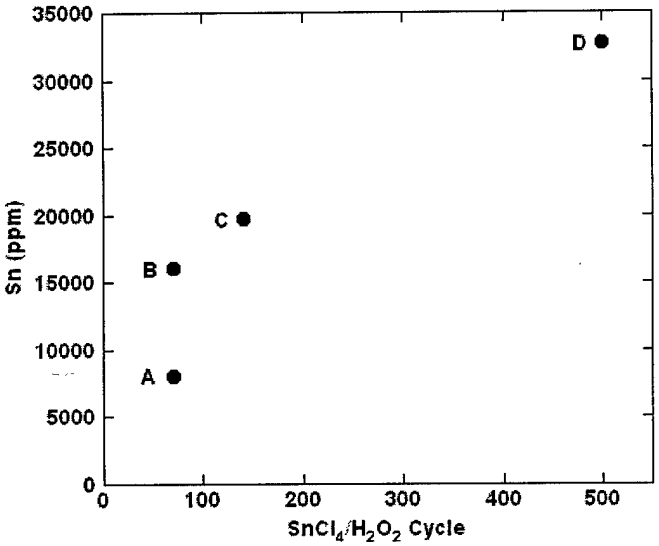

Figure 3 ICP analysis of Sn content in SnO_2 coated ZrO_2 particles.

The ICP-AES also provides information about the growth parameters. For example, Samples A and B are both after 70 $SnCl_4/H_2O_2$ cycles at 250 °C, but Sample B has approximately twice the concentration of Sn as Sample A. Samples A and B were grown under different conditions. Sample A received 2 second precursor doses while Sample B received 3 second precursor doses. This could suggest that the individual surface reactions are not saturating and longer doses lead to higher growth rates. The data could also be explained by the longer precursor doses better facilitating nucleation. Another interesting observation is the change in concentration from Sample B to Sample C. Sample C (140 $SnCl_4/H_2O_2$) had twice the number of reaction cycles as Sample B (70 $SnCl_4/H_2O_2$). Samples B and C were grown under the same growth conditions using 3 second precursor exposures. Despite the similar conditions and twice as many cycles, Sample C had only 23% more Sn. Sample C was obtained by further depositing on Sample B. While removing a portion of Sample B, the reactor was cooled down to room temperature. Consequently, there was a long delay after 70 cycles. It is possible that the surface species are not stable for long periods of time on the SnO_2 surface. The long delay could have resulted in a loss of the reactive surface species on the SnO_2 surface and required renucleation. This could explain the lower than expected Sn concentration after 140 $SnCl_4/H_2O_2$ cycles.

Transmission electron microscopy was done on a Philips CM10 100 kV transmission electron microscope. Figure 4 shows TEM images of uncoated ZrO_2 particles (4a), and ZrO_2 particles

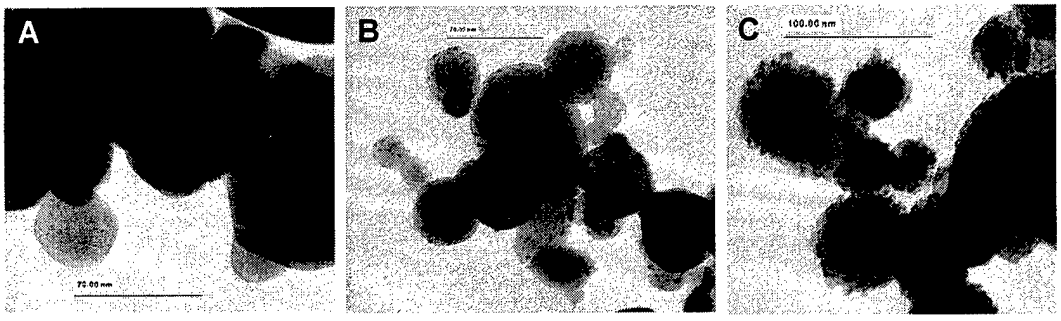

Figure 4 TEM images of A) uncoated ZrO_2, B) 140 cycles of SnO_2, and C) 500 cycles of SnO_2.

after 140 (4b) and 500 (4c) $SnCl_4/H_2O_2$ cycles. The TEM image shown in Figure 4a reveals ZrO_2 particles with smooth surfaces. The TEM image in Figure 4b reveals particles with a partially roughened surface. Additionally, dark areas are observed on these particles. Figure 4c displays a TEM image of particles with very rough surfaces. These TEM images are consistent with the nucleation and deposition of a rough SnO_2 film on the ZrO_2 particles.

The ZrO_2 particles of this study are fully oxidized. In contrast, the aluminum particles from Technanogy are only partially oxidized. These particles consist of an Al core with an Al_2O_3 shell. It is important that the Al particles do not further oxidize during the SnO_2 deposition. Thermo-gravimetric analysis (TGA) was used to observe the oxidation properties of the Al particles (Figure 5). Untreated Al particles from Technanogy were analyzed. Aluminum particles were also heated to our reaction temperature of 250 °C in the presence of N_2 flow. A final sample was heated to 250 °C under N_2 flow and exposed to H_2O_2. The H_2O_2 exposures were similar to H_2O_2 exposures used during 100 reaction cycles. TGA experiments showed that all three of the samples did not oxidize in air until at least 400 °C. These experiments suggest that the Al particles from Technanogy should not have a problem with oxidation under the growth conditions necessary for the deposition of SnO_2 using $SnCl_4$ and H_2O_2.

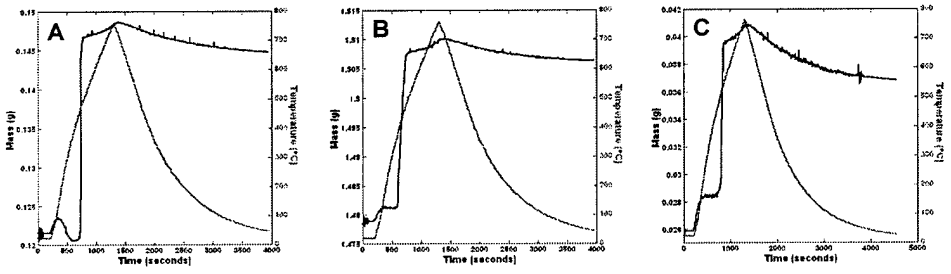

A) Technanogy Al powder untreated
B) Technanogy Al powder after 150 minutes at 250°C under N_2 flow
C) Technanogy Al powder after 100 H_2O_2 doses at 250°C

Figure 5. Thermogravimetric data on as received Al particles and processed Al particles.

The aluminum nanoparticles were obtained from Technanogy and are approximately 50 nm in diameter. The TEM image shown in Figure 6 reveals a core aluminum particle surrounded by a smooth oxide layer. The aluminum nanoparticles were coated with SnO_2 using parameters derived from the SnO_2 deposition on the ZrO_2 particles. Ultimately, it was determined that the deposition performed at 250 °C provided inadequate deposition. Subsequently, the deposition temperature was increased to 350 °C. Figure 7 shows a TEM image after 400 reaction cycles at 350 °C. The TEM image reveals a particle with a much roughened surface in contrast to the smooth surfaces observed on the uncoated particles in Figure 6. The roughened surface is consistent with the deposition of a rough SnO_2 film on the aluminum nanoparticles. Small portions (~0.02 g) of the coated particles were detonated with a Tesla coil to test for explosive properties. The detonation of the particles produced a bright flash. Figure 8 shows a picture of this flash captured from a digital video recorder.

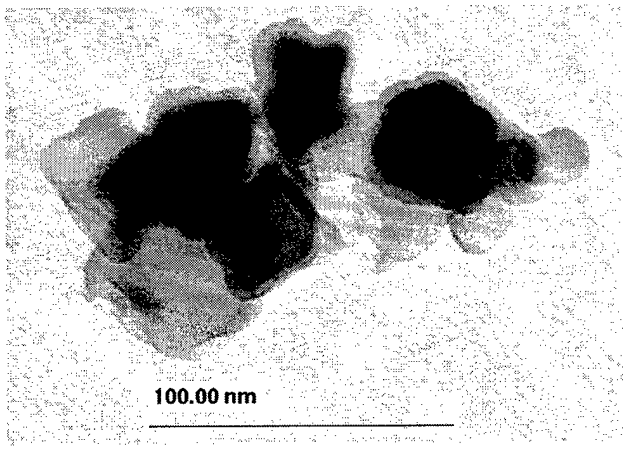

Figure 6 TEM image of Technanogy Al particle, as received.

The detonation of the SnO_2-coated Al particles was monitored and recorded with a digital camcorder. Six sequential frames from this detonation are displayed in Figure 8. The frames were recorded at a rate of ~30 frames per second. For comparison purposes, uncoated Al particles were also detonated and recorded in a similar manner. Figure 9 displays various frames from these results. The frame shown at a time of 0.968 seconds represents the brightest glow. Overall, the detonation of the uncoated Al particles proceeds over a time period of over six seconds. These detonation results show that the SnO_2-coated Al particles detonate much more rapidly than the uncoated Al particles.

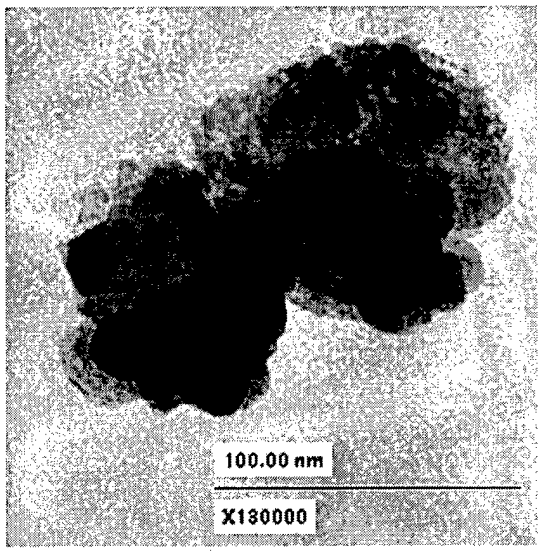

Figure 7 TEM image of Al particle with 400 cycles of SnO2 ALD chemistry.

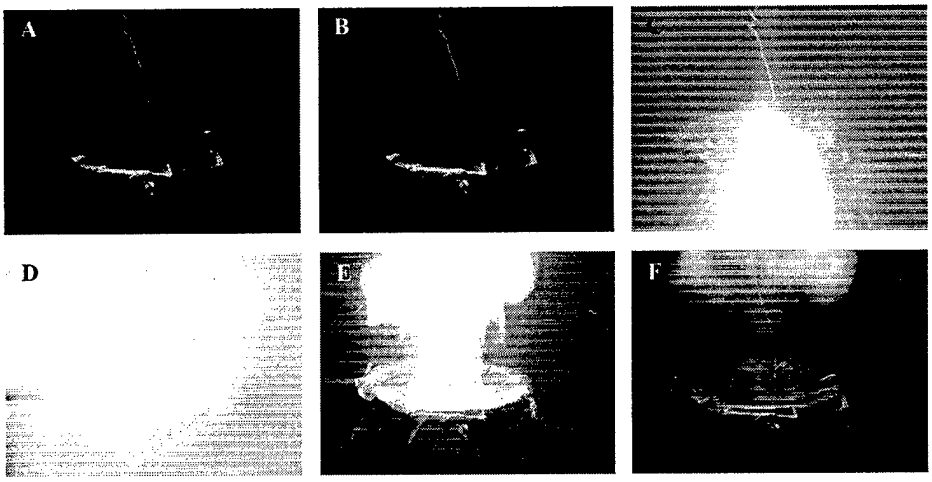

Figure 8. Sequential frames from digital video recording (30 frames/sec) of the ignition of SnO_2 coated Al nanoparticles.

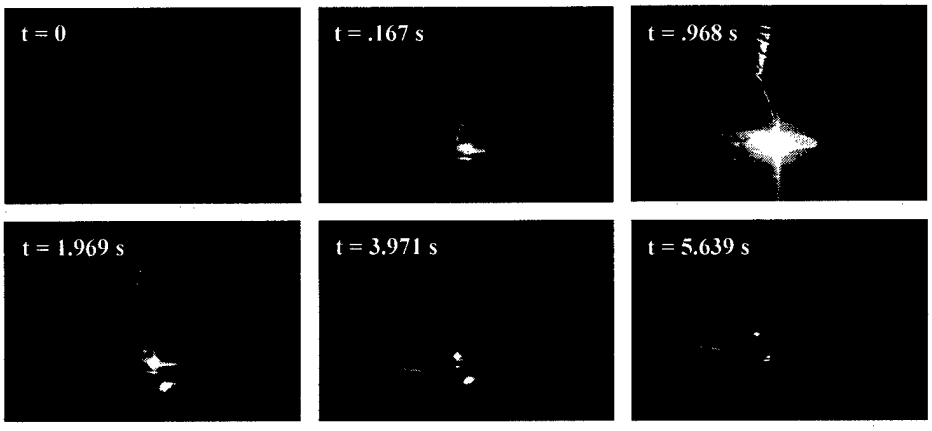

Figure 9. Selected frames from digital video recording (30 frames/sec) of the ignition of Al nanoparticles.

Inductively coupled plasma atomic emission spectroscopy was used to determine the stoichiometry of SnO_2-coated Al particles. These results are summarized in Table 1. The following reaction can be used to estimate the optimum ratio of SnO_2 to Al:

$$3\ SnO_2 + 4\ Al \rightarrow 3\ Sn + 2\ Al_2O_3$$

Using the molecular weights of SnO_2 and Al only, a stoichiometric mixture of SnO_2 and metallic Al would be 69.5% Sn by mass. The Al particles used in this study consisted of an Al core with Al_2O_3 coating. The particles had an average diameter of 51.2 nm and an oxide thickness of 3.4 nm. The Al core consists of 61.1% mass of the total particle. Considering the particles used in this study, the SnO_2-coated Al particles should contain 62.3% mass Sn. The results shown in Table 1 reveal that the Sn concentrations for a variety of conditions are in the range of 1.8 – 10.4%. These Sn concentrations are very low compared to the calculated 62.3% mass of Sn for the optimized SnO_2 coating on the Al particles.

Sample	Precursor dose time (s)	Number of Cycles	Temperature (°C)	Sn (% mass)
1	3	250	250	10.4
2	3	250	250	9.1
3	3	250	250	4.0
4	3	250	250	6.9
5	3	250	250	3.4
6	3	350	250	4.2
7	1	400	250	7.4
8	2	400	350	1.8
9	1	400	350	4.6
10	1	500	350	2.8
11	1	500	350	7.2
12	1	500	350	4.1
13	1	1000	350	2.9

Table 1. Summary of SnO_2 trials on nanosized Al particles.

The reported growth rate for the atomic layer deposition of SnO_2 using $SnCl_4$ and H_2O_2 is ~ 0.3 Å/AB cycle at growth temperatures of 250 – 400 °C. The growth temperatures used in this study were 250 or 350 °C. Under these conditions, a stoichiometric amount (62.3% mass) of SnO_2 should be deposited with ~230 $SnCl_4/H_2O_2$ reaction cycles. The measured Sn concentrations of 1.8 – 10.4% could indicate a nucleation problem during the SnO_2 deposition on the Al particles. The particles are terminated with an Al_2O_3 surface. If this surface is contaminated or is nonfunctionalized, the nucleation of SnO_2 on the Al_2O_3 surface could be greatly hindered.

A sample of the SnO_2 coated Al particles was sent to Los Alamos National Laboratory for testing by Steven Son and coworkers. The particles were coated at 350 °C using 500 $SnCl_4/H_2O_2$ reaction cycles. One of the experiments conducted at Los Alamos National Laboratory consisted of measuring pressure versus time during ignition of the SnO_2-coated Al particles in a small closed vessel. The pressure increase as a result of the ignition is proportional to the stored

energy in the energetic material. The pressure increases observed during the ignition of the SnO_2-coated Al particles were only 3 – 5 % of their optimized energetic materials.

Unpublished results by Steven Son and coworkers examined the pressure increase for a range of stoichiometries in the Al/WO_3 energetic material system. These results show that decreasing the O/Al mole ratio from 1.5 to 1.0 decreases the pressure increase from the maximum by ~72%. The SnO_2-coated Al sample that was examined had a Sn concentration of 7.2% by mass. Assuming that the Sn is in the form of SnO_2, this corresponds to an O/Al mole ratio of 0.28. Based on this O/Al mole ratio, it is not surprising that the pressure increase during ignition of the SnO_2-coated Al particles was so relatively low.

Increasing the O/Al mole ratio (increasing the SnO_2 concentration) would likely improve the properties of the energetic SnO_2-coated Al particles. In contrast to SnO_2 deposition on ZrO_2 particles, the SnO_2 concentration on Al particles was not strongly correlated to the number of reaction cycles. The SnO_2 concentration was more likely controlled by nucleation. Improving the nucleation of the SnO_2 on the Al particles would provide much more control of the stoichiometry of the SnO_2 and Al. As a result, the energetic properties of the SnO_2-coated Al particles could be optimized.

The nucleation of SnO_2 on the Al particles could be improved by placing a thin layer of Al_2O_3 on the Al particles using atomic layer deposition. Although the Al particles are already terminated with a thin Al_2O_3 layer, it could be nonfunctionalized or contaminated. Al_2O_3 films grown using $Al(CH_3)_3$ and H_2O have been well studied. These films have been thoroughly characterized over a wide range of growth parameters. Additionally, Al_2O_3 films deposited using $Al(CH_3)_3$ and H_2O nucleate well on a variety of substrates including oxides, nitrides, metals and polymers. The atomic layer deposition of Al_2O_3 on the Al particles could be accomplished with only minor modifications of the current reactor setup.

Design of Pilot Facility

The ALD coating of particles has many applications in niche small volume markets (less than 100,000 lb/yr annual production needs) which includes the formation of composite thermite particles. This being the case, there are few size differences between the pilot facility designed here and the anticipated full scale production facility. A schematic of the proposed system is shown in Figure 10. Additionally, the costs projected in this report are for the coating of the particles only. They do not include the purchase of the substrate particles.

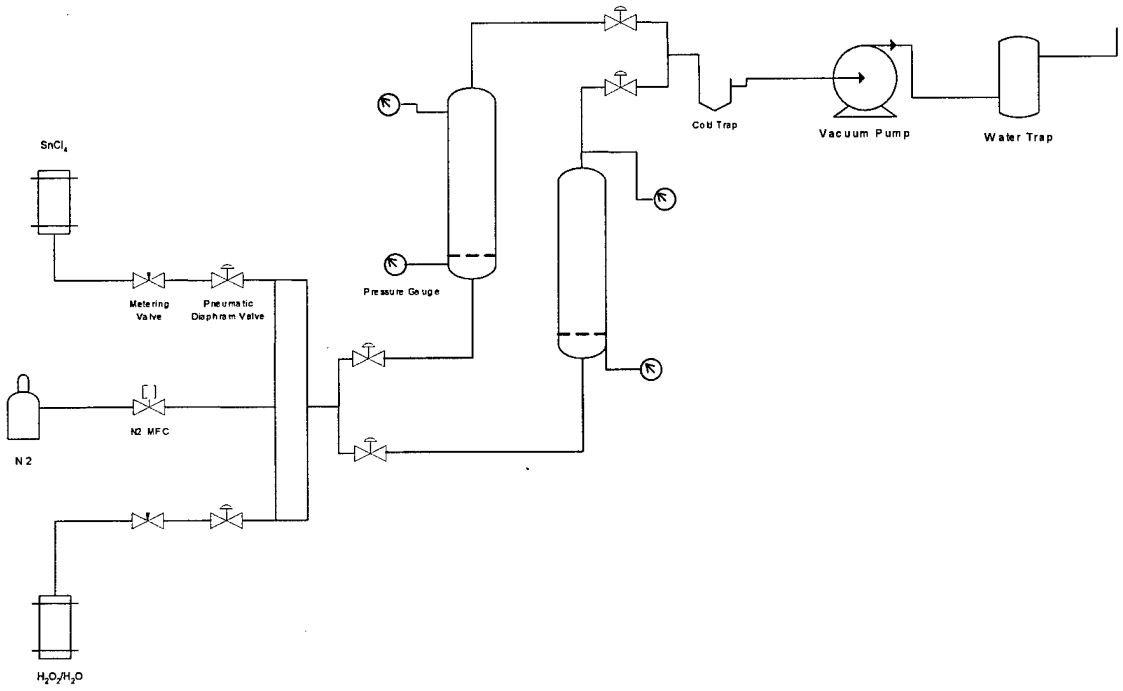

Figure 10. Schematic for Pilot Scale ALD Fluidized bed coating system.

Capital Cost Estimation

Capital cost estimation for this project began with sizing all of the necessary equipment. The fluidized bed size is approximated using a number of different factors and sources, including annual production amounts and batch run times (3 hours for 240 cycles). An appropriate fluidized bed size is approximated to be .65 m in diameter and 2.25 m tall. These dimensions are used to determine cost from a 2002 vessel cost chart [17]. A number of different expenses are added to the cost of the vessel, including costs for the porous metal distributor plate, the pulsed blow-back filters, as well as welding and machining costs. Each fluidized bed reactor is estimated to cost $10,000.

Other pieces of equipment that needed to be sized are piping and valves along with the vacuum pump, cold trap, and water trap. The piping used on the reactant side is ¼" stainless-steel tubing; the same used on the experimental scale reactor. The only draw back this may cause is somewhat longer dose times than expected due to the flow limitations of the pipe diameter. The vacuum side of the reactor will use NW 25 ISO-KF quick assembly vacuum tubing with an inside diameter of almost 1 inch. This will allow for maximum flow to the vacuum pump. All valves on the reactant portion of the system are identical to the hardware used in the experimental setup. The experimental setup uses pneumatically-actuated, bellows-enclosed

diaphragm valves, which are both reliable and provide protection from the harsh reactants. The pneumatic valves used on the vacuum side are ½", high-flow, Swagelok VCR valves, with two used in parallel if the flow rate through the valves is too low.

The semiconductor industry uses chemicals similar in nature to the ones used in the ALD coating of particles. Thus, the vacuum equipment which has been proven in this industry will be mimicked in this application. The pump chosen is a dry screw pump, which overcomes a few of the drawbacks of normal oiled pumps used in the current experimental systems. The unit has a pumping speed of 77 L/min, which will be sufficient for pulling vacuums quickly on the system. The pump is one of the most expensive pieces of equipment for the system at $18,000.

Heating for the fluidized bed reactor will be provided by a clam-shell type low temperature furnace. There are many companies which offer large furnaces such as this with maximum temperatures up to 1200 °C for a reasonable price. It is estimated that the cost of furnaces that can take a tube as large as our fluidized bed and meet our maximum temperature requirement of 500 °C will cost approximately $20,000.

The two remaining pieces of equipment on the system are the cold trap and water trap. Both pieces of equipment cost under $5000, and both are needed to minimize pollution and emissions. While all reactants and HCl byproducts should be condensed in the cold trap, the water trap is the second line of defense. Total capital cost for the system equals $500,000. Estimated construction time for this plant, including lead-time and custom fabrication, is one year. This length of time is used in the economic model. A comprehensive list of necessary equipment, along with a utilities summary, can be seen in Table 2.

Equipment Name	Utility Requirements
Fluidized Bed	None
Vacuum Pump	1.9 kW electricity
Cold Trap	Liquid N2
Water Trap	None
Pneumatic Valves	Compressed Air
Needle Valves	None
Mass Flow Controller	Low voltage control signal
Furnace w/ control	5 kW electricity
Other plumbing components	None
Pulsed Filters	Inert gas
Vibrational Motors	1.3 kW
Computer Control	300 W electricity

Table 2. Summary of Equipment and Utility Requirements.

Operating Costs

This project has a number of associated variable costs. Factors composing these costs are reactants, electricity, waste disposal, and analytical tests. The waste disposal cost is considered insignificant in the economic analysis because the very small amount of waste disposed is that

from the cold and water traps. Electricity requirements are quite small for the process. Electricity costs are $0.024/kg of product, which relates to an annual expenditure of $2400. Reactants account for approximately 25% of all variable costs. Tin tetrachloride makes up most of this cost with a wholesale price of $10/lb, which translates to $0.041 per kilogram of product. Hydrogen peroxide solution ($0.53/lb) and nitrogen costs a combined total of $0.01 per kilogram of product. Analytical methods make up the bulk of the variable costs. TEM images are $0.048/kg of product. LECO and ICP tests have a combined cost of $0.078/kg of product. The total annual variable costs are approximately $19k per year, or $0.19/kg of product.

Fixed operating costs of the proposed design have also been analyzed. It is estimated that the nominal 100,000 lbs/year production scheme can be run by two operators, working 8 hours a day, 5 days a week for twelve months (2000 operating hours). The operators are estimated to have annual salaries of $35k. A number of cost factors have been used to approximate supervising wages, overhead costs, and maintenance costs. These factors were set to simulate reasonable expenditures. The fixed operating costs are $261k annually, or $2.61/kg product.

Selling prices per pound have been computed for zero profit as seen in the table below.

Annual Production Rate (kg/year)	Selling price ($/kg)
10K	23.92
100K	4.37
500K	1.78

Table 3: Break-even selling prices.

These values give an estimate of what selling prices need to be in order to break-even. As the annual production rate increases, the selling price needed to break-even decreases.

Case Studies

Net present value is the value of an investment's future cash flow minus the initial investment cost. The following evaluations were made for nominal operating conditions of 100,000 kg/year and 240Å coatings. The net present value of the proposed plant is around $1.62MM over 15 years. This results in an efficient return on the initial venture guidance appraisal estimate of a $500M investment. A venture guidance appraisal serves to provide a fairly accurate estimate of investment costs by accounting for various aspects of the construction process. The investor's rate of return (IRR) is effectively the compound annual rate of return realized on the investment. The feasibility of this process is illustrated in the IRR, which is found to be 50.0%.

Case studies were carried out for varying annual production rates of 10, 100, and 500 thousand kilograms per year. A table summarizing these case studies can be seen below.

Annual Capacity (kg)	Selling Price ($/kg)	NPV ($MM)
10,000	$ 71.00	1.52
100,000	$ 9.37	1.62
500,000	$ 2.92	1.83

Table 4: Case analyses results table.

In these case studies, all calculations are based on an IRR of 50%. A 50% IRR is considered acceptable by specialty chemical manufacturers. The annual production rate does have a significant effect on the selling price. The 10k production rate results in a selling price of around $71/kg. This selling price is much higher than either the 100K or 500K production rate price. The 100K and 500K production rates result in maximum selling prices of $9.37 and $2.92 respectively for the 240 Å film thicknesses.

Sensitivity Analysis

A sensitivity analysis has been performed to see how the economic feasibility of this project changes with variations in the capital cost, fixed operating cost, and variable operating cost. The following sensitivity analysis demonstrates how fluctuations in costs will affect the company. The following graphs are for the 100K/year batch.

The first graph shows how the selling price varies for breakeven and 50% IRR value as the capital costs fluctuate by ±40%.

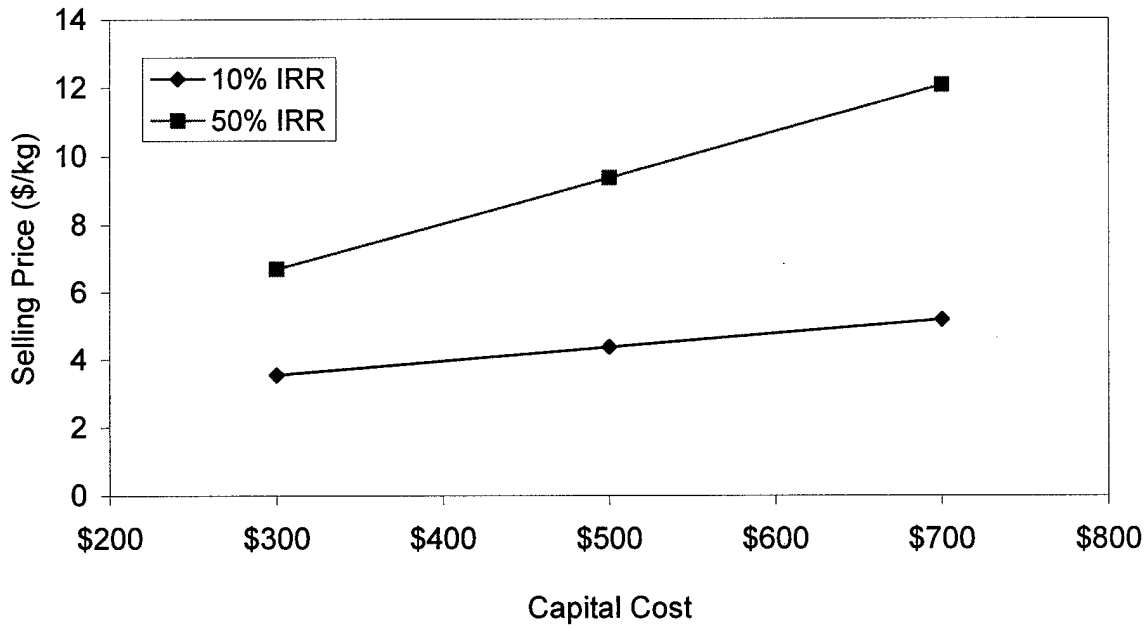

Figure 11. Selling Price vs. Capital Cost (± 40%) for a given IRR and 100,000 kg/yr production capacity.

As seen in the graph, the selling price fluctuates more for changes in capital costs at higher IRR values. For an IRR value of 50%, the selling price ranges from just below $7 to just over $12 for the fluctuation in capital costs. However, for an IRR value of 10%, the selling price varies by only about $2.

The next graph shows how the selling price varies for various IRR values as the operating costs fluctuate by ±40%.

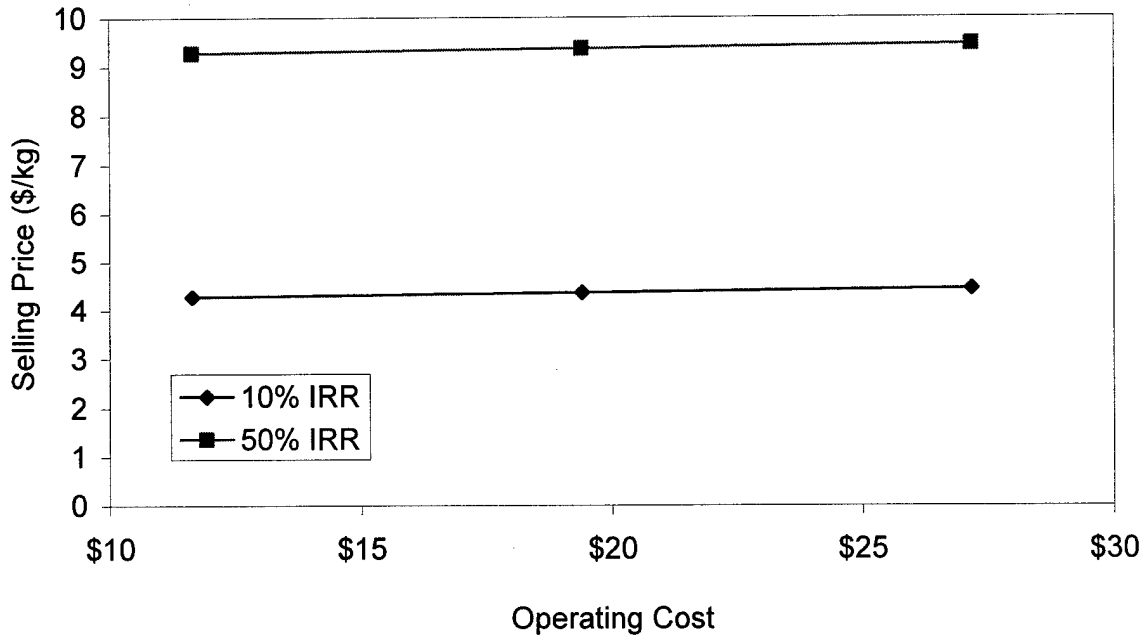

Figure 12. Selling Price vs. Operating Costs (± 40%) for a given IRR and 100,000 kg/yr production capacity.

Fluctuations in the operating costs do not cause the selling price to vary as much as fluctuations in the capital costs. For an IRR value of 50%, the selling price has varies from $9.28 to $9.45, which is a range of $0.17. The selling price at an IRR value of 50% for changes in capital costs varies from $6.69 to $12.05, which is a range of $5.36. As one can see, fluctuations in capital costs will have a greater influence of the selling price than fluctuations in operating costs will have. The same trend exists for the operating costs that exist for the capital costs; as the IRR value increases, the selling price will have a larger range as the costs vary.

Fluctuations in fixed costs were investigated as well. Figure 13 shows the variation in selling price with fixed cost. For an IRR value of 50% the selling price varies from $8.06 to $10.68. This is a more significant change than what is caused by operating costs, however not as great as the capital expenses or the largest variation the capacity changes.

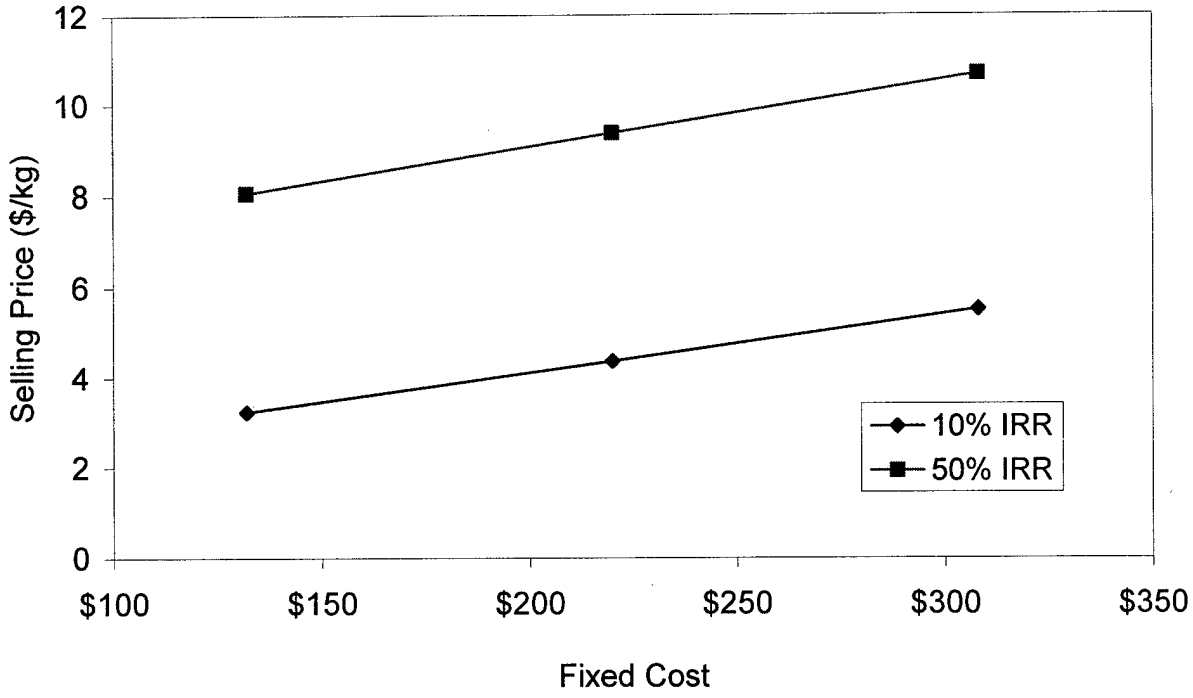

Figure 13. Selling Price vs. Fixed Costs (± 40%) for a given IRR and 100,000 kg/yr production capacity.

The IRR vs. selling price was also plotted to demonstrate the relationship how the selling price varies.

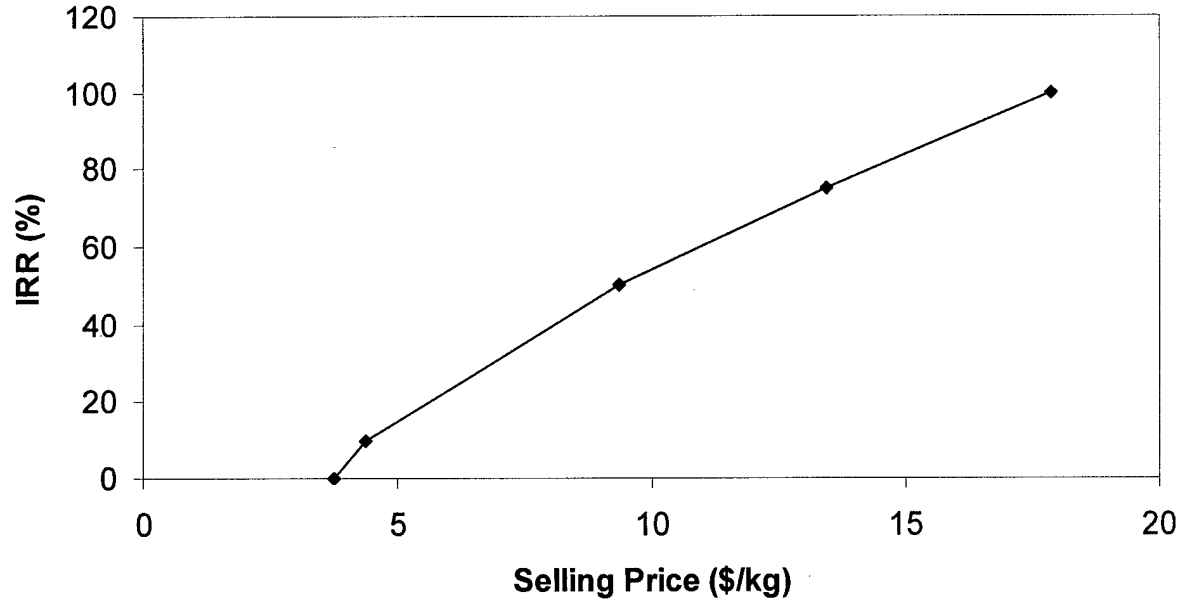

Figure 14. IRR vs. Selling Price.

An almost linear relationship exists between the IRR and the selling price. At higher IRR values the relationship is linear while at low IRR values the relationship isn't linear.

Conclusions

Films of oxidizers such as SnO_2 can be grown onto nanosized particulate substrates. The metallic substrates for thermite do accept the oxidizer coatings however, not as well as the oxide particles, which are more conventionally studies for ALD. It is believed that some surface contaminant or incomplete functionalization of the surface of the aluminum particles caused the lower observed rates of film growth. This can likely be overcome with a few cycles of alumina growth from trimethyl aluminum and water.

The composite thermite particles were tested for reactivity through both qualitative and quantitative means. A small sample of both the aluminum and the composite particles were ignited with a tesla coil and the resulting reaction was video taped with a hand held digital video camera. The composite particles produced a much faster and violent reaction when compared with the uncoated aluminum particles.

The pressure increases observed during the ignition of the SnO_2-coated Al particles were only 3 – 5 % of their optimized energetic materials. The material tested has an O/Al molar ratio of 0.28, much lower than the stoichiometric 1.5 ratio for the thermite reaction. As these materials become less chemically ideal, the energy release falls off rapidly, explaining the low releases observed in this study.

A system has been designed for the larger scale production of ALD coated particles. For a relatively minimal investment of $500,000 a system capable of coating 100,000 kg of aluminum particles per year can be constructed.

The economic case studies provide some useful insight into the economic variations of the process. Annual production rate drastically affects the selling price needed to retain a 50% IRR. When producing only 10,000 lbs/year, the selling price must be $71/kg. This price is much greater than the 100,000 lbs/yr and 500,000 lbs/yr selling prices of $9/kg and $3/kg, respectively. The sensitivity analysis also provides useful insight into how cost variations will affect the selling price.

Recommendations for Future Work

It is the belief of the authors that the results provided here are very promising. This line of research should be continued to fully develop the use of atomic layer deposition for creating composite materials. It would be useful to pursue two parallel tracks for this continued work; 1) continue the development of the oxidizer chemistry onto aluminum particles and 2) prove that atomic layer deposition can be achieved on particles at large scale.

The non-idealities observed when the tin oxide films were grown on the aluminum particles as opposed to the zirconia particles need to be resolved. The resolution of this issue could be as simple as the addition of 5-10 cycles of alumina ALD chemistry to build a good tie layer on the

surface of the aluminum particles. Further characterization of these films to their barrier properties would also provide good information on the long term stability of the composite particles. Additional chemistries such as MoO_3 with higher theoretical energy content should also be investigated.

On a similar track, the scale-up of atomic layer deposition needs further investigation. It has been achieved in fluidized beds on the 100 g scale. It will not be fully scalable until it has been successfully performed in multi-kg batch sizes. It is suggested that this be performed on non-reactive demonstration systems which also have commercial applications. Potential systems for this demonstration would be alumina on boron nitride for electronic packaging filler materials applications or tin oxide on barium titanate for semiconductor applications.

Publications Resulting from this Work

Ferguson, J., George, S., Buechler, K., Weimer, A., "*Fabrication of Composite Thermite Nanoparticles through Atomic Layer Deposition*", in **Proceedings of the Annual Meeting of the American Institute of Chemical Engineers**, 2003.

Persons Involved in this Work

Karen Buechler, ALD NanoSolutions, Inc.
John Ferguson, University of Colorado
Steven George, ALD NanoSolutions, Inc. and University of Colorado
Steven Son, Los Alamos National Laboratory
Alan Weimer, ALD NanoSolutions, Inc. and University of Colorado

Acknowledgements

The authors would like to thank Dr. Steven Son and co-workers at Los Alamos National Laboratory for their testing of the composite particles.

This material is based upon work supported by the Air Force Office of Scientific Research under Contract No. F49620-02-C-0058. Any opinions, findings and conclusions or recommendations expressed in this material are those of the authors and do not necessarily reflect the views of the Air Force Office of Scientific Research.

References

1. Terry Lowe, *The Revolution in Nanometals*, Advanced Materials & Processes, January 2002, p. 63.
2. T.M. Tillotson, A.E. Gash, R.L. Simpson, L.W. Hrubesh, J.H. Satcher, Jr. and J.F. Poco, *Nanostructured Energetic Materials using Sol-Gel Methodologies*, J. Non-Cryst. Solids **285**, 338 (2001).
3. C.E. Aumann, G.L. Skofronick and J.A. Martin, *Oxidation Behavior of Aluminum Nanopowders,* J. Vac. Sci. Technol. B **13**, 1178 (1995).

4. M.E. Brown, S.J. Taylor and M.J. Tribelhorn, *Fuel-Oxidant Particle Contact in Binary Pyrotechnic Reactions*, Propellants, Explosives, Pyrotechnics **23**, 320 (1998).
5. S.M. George, A.W. Ott and J.W. Klaus, *Surface Chemistry for Atomic Layer Growth*, J. Phys. Chem. **100**, 13121 (1996).
6. M. Ritala and M. Leskela, *Atomic Layer Deposition*, in **Handbook of Thin Film Materials**, H.S. Nalwa, Editor, Academic Press, San Diego (2001) Vol. 1, Chap. 2.
7. J.D. Ferguson, A.W. Weimer and S.M. George, *Atomic Layer Deposition of Ultrathin and Conformal Al_2O_3 Films on BN Particles*, Thin Solid Films **371**, 95 (2000).
8. J.D. Ferguson, A.W. Weimer and S.M. George, *Atomic Layer Deposition of SiO_2 Films on BN Particles Using Sequential Surface Reactions*, Chem. Mater. **12**, 3472 (2000).
9. J.R. Wank, S.M. George and A.W. Weimer, *Vibro-fluidization of Fine Boron Nitride Powder at Low Pressure*, Powder Technology **121**, 195 (2001).
10. L.L. Wang, Z.A. Munir and Y. M. Maximov, *Thermite Reactions: Their Utilization in the Synthesis and Processing of Materials*, J. Mater. Sci. **28**, 3693 (1993).
11. S.H. Fischer and M.C. Grubelich, *Theoretical Energy Release of Thermites, Intermetallics and Combustible Metals*, SAND98-1176C, 24th International Pyrotechnics Seminar, Monterey, CA, July 1998.
12. M. Utriainen, M. Kroger-Laukkanen and L. Niinisto, *Studies of NiO Thin Film Formation by Atomic Layer Epitaxy*, Mater. Sci. Eng. B **54**, 98 (1998).
13. P. Tagtstrom, P. Martensson, U. Jansson and J.O. Carlsson, *Atomic Layer Epitaxy of Tungsten Oxide Using Oxyfluorides as Metal Precursors*, J. Electrochem. Soc. **146**, 3139 (1999).
14. H. Seim, M. Nieminen, L. Niinisto, H. Fjellvag and L.S. Johannson, *Growth of $LaCoO_3$ Thin Films from β-diketonate Precursors*, Appl. Surf. Sci. **112**, 243 (1997).
15. O. Nilsen, M. Peussa, H. Fjellfab, L. Niinisto and A. Kjekshus, *Thin Film Deposition of Lanthanum Manganite Perovskite by the ALD Process*, J. Mater. Chem. **9**, 1781 (1999).
16. H. Viirola and L. Niinisto, *Controlled Growth of Tin Dioxide Thin Films by Atomic Layer Epitaxy*, Thin Solid Films **249**, 144 (1994).
17. M. Peters, K. Timmerhaus, R. West, **Plant Design and Economics for Chemical Engineers**, McGraw-Hill Science/Engineering/Math; 5th Edition, 2002.